The Theory of the Reverse Diffusion of Ions in Mixed Electrolyte Solutions and Experimental Results on the HCl-$CaCl_2$-H_2O Ternary System[1)]

Masayuki NAKAGAKI and Shuji KITAGAWA

Faculty of Pharmaceutical Sciences, Kyoto University, Sakyoku, Kyoto 606

(Received October 13, 1975)

Reverse diffusion is the migration of solutes in the direction opposite to that expected from the concentration gradient, that is, from a portion with a lower concentration to that with a higher concentration. This type of diffusion of ions in mixed electrolyte solutions was studied theoretically on the basis of nonequilibrium thermodynamics. For a solution containing two kinds of cations and one kind of anion, it has been concluded that the reverse diffusion occurs when the mobilities of the coexisting ions differ largely, because the effect of the diffusion potential is pronounced in such a case. It has also been concluded that the practical diffusion coefficient of an ion varies linearly with the ratio of the concentration gradient of a coexisting ion to that of the diffusing ion when the average concentration ratio of the ions is fixed. Moreover, the range of the concentration-gradient ratio, where the practical diffusion coefficient is negative, has been determined. These theoretical conclusions were tested experimentally for the HCl-$CaCl_2$-H_2O ternary system. The results satisfactorily verified that reverse diffusion actually occurred and that the relationship between the diffusion coefficient and the concentration-gradient ratio was linear, as has been expected.

The Fick law of diffusion predicts that a solute will migrate from a portion with a higher concentration to one with a lower concentration at a rate proportional to the concentration gradient. The diffusion through a membrane, that is, the so-called passive transport, also proceeds in the same direction. In contradiction to this, the active transport in biological membranes is transport against the concentration gradient. However, an ion can migrate against its concentration gradient passively in a system of mixed electrolytes, at least under certain limited conditions. This has already been pointed out theoretically in our previous paper.[2)]

According to nonequilibrium thermodynamics, the flux of the ion (i), J_i, is proportional to the gradient of the total potential of the component, $\tilde{\mu}_i$, which is the electrochemical potential in the present case. Thus, the rate of the diffusion of each ion is modified by the effect of the electric potential, the so-called diffusion potential, and, under certain conditions, the reverse diffusion of an ion can proceed, as has already been predicted both qualitatively[3)] and quantitatively.[2,4)] However, no precise experimental support of the reverse diffusion has so far been given. For the KCl-$MgCl_2$-H_2O system and the K(HAsp)-$Mg(HAsp)_2$-H_2O system, where $HAsp^-$ indicates the hydrogen aspartate anion, it has been reported[5)] that the diffusion coefficient of a cation becomes smaller with the addition of a faster cation, but the diffusion coefficient has not reached a negative value.

Theoretical

Practical Diffusion Coefficient of Ions. According to nonequilibrium thermodynamics, the flux of the ion (i), $[J_i]$ (mg-ion·cm^{-2}·s^{-1}), through a diffusion layer between two aqueous solutions, I and II, is given by the following equation,[2,4,6,7)] after the term of the electric potential gradient has been eliminated by using the condition that the diffusion current is zero in the steady state:

$$[J_i] = -D_i\left(\frac{\partial[i]}{\partial x}\right) + \frac{z_i B_i [i]}{\sum_j z_j^2 B_j [j]} \sum_j z_j D_j \left(\frac{\partial [j]}{\partial x}\right) \quad (1)$$

Here, $[i]$ (g-ion·l^{-1}) is the concentration of the i ion, while x is the coordinate taken in the direction of the flux. Moreover, B_i is the mobility of the ion, i, which is related to the radius of the ion, a_i, and the viscosity of the medium, η, by the Stokes law if the ion is considered to be spherical;

$$B_i = 1/6\pi\eta a_i \quad (2)$$

and D_i is the diffusion coefficient related to the mobility by the following equation:

$$D_i = kTB_i h_i \quad (3)$$

where k is the the Boltzmann constant, T is the absolute temperature, and h_i is the coefficient;

$$h_i = 1 + (\partial \ln f_i / \partial \ln [i]) \quad (4)$$

with f_i being the activity coefficient of the ion, i. If the concentration dependence of the activity coefficient can be neglected so that $h_i=1$, then Eq. 3 is simplified to:

$$D_i = kTB_i \quad (5)$$

which gives the Einstein equation when Eq. 2 is used together with it.

The actual rate of diffusion of the ion, i, in a solution, however, can not be determined by D_i or, in other words, by the ionic radius and the solvent viscosity only, because of the electrostatic interaction between ions, or, we could say, because of the effect of the diffusion potential. The practical diffusion coefficient of the ion (i), D'_i, may then be defined by:

$$[J_i] = -D_i'(\partial[i]/\partial x) \quad (6)$$

Its theoretical expression is given by the following equation, which has been derived from Eq. 1, in the same approximation as was used for Eq. 5:

$$D_i' = kTB_i\left\{1 - \frac{z_i[i]\sum_j z_j B_j(\partial[j]/\partial x)}{(\sum_j z_j^2 B_j[j])(\partial[i]/\partial x)}\right\} \quad (7)$$

In the case of an electrolyte solution containing one cation, 1, and one anion, 3, only, Eq. 7 gives the Haskell

equation:

$$D_1' = D_3' = kT(z_1+|z_3|)B_1B_3/(z_1B_1+|z_3|B_3) \quad (8)$$

If, however, the electrolyte solution contains two cations, 1 and 2, and one anion, 3, the practical diffusion coefficients are given, on the basis of Eq. 7 and the equation of electrical neutrality;

$$z_1[1] + z_2[2] = |z_3|[3] \quad (9)$$

by the following equations:

$$D_1' = kTB_1\left\{1-z_1\frac{F(1/2)}{G(1/2)}H\right\} \quad (10a)$$

$$D_2' = kTB_2\{1-z_2H\} \quad (10b)$$

$$D_3' = kTB_3\left\{1+|z_3|\frac{1+G(1/2)}{1+F(1/2)}H\right\} \quad (10c)$$

where:

$$H = \frac{(B_2-B_3)+(B_1-B_3)G(1/2)}{(z_2B_2+|z_3|B_3)+(z_1B_1+|z_3|B_3)F(1/2)} \quad (10d)$$

Here, $F(i/j)$ is the ratio of concentrations (g-equiv·l^{-1});

$$F(i/j) = |z_i/z_j|\cdot[i]/[j] \quad (11)$$

and $G(i/j)$ is the ratio of the concentration gradients, the concentration being expressed again in g-equiv·l^{-1}:

$$G(i/j) = |z_i/z_j|\cdot(\partial[i]/\partial x)/(\partial[j]/\partial x) \quad (12)$$

Equations 10a—d show that the practical diffusion coefficient, D'_i, is a function of the concentration ratio and the concentration-gradient ratio, and that D'_2 is linear and D'_1 and D'_3 are hyperbolic against $G(1/2)$ at a fixed $F(1/2)$. As for the 3 anion, Eqs. 10c, d may be rewritten, by using Eq. 9, as follows:

$$D_3' = kTB_3\left\{1+|z_3|[1+F(1/2)]\right.$$
$$\left.\times\frac{(B_2-B_3)+(B_1-B_2)G(1/3)}{(z_2B_2+|z_3|B_3)+(z_1B_1+|z_3|B_3)F(1/2)}\right. \quad (13)$$

Therefore, D'_3 is linear with $G(1/3)$ at a fixed $F(1/2)$.

Reverse Diffusion. As is obvious from Eq. 6, the reverse diffusion of the ion, i, takes place when the practical diffusion coefficient, D'_i, is negative; the condition for it is readily obtained from Eqs. 10a—d:

When the 1 cation is also present, the reverse diffusion of the 2 cation proceeds when Eq. 14 is fulfilled if $B_1>B_3$, or when Eq. 15 is fulfilled if $B_1<B_3$:

$$G(1/2) > \frac{(z_1/z_2)(B_1/B_3)+(|z_3|/z_2)}{(B_1/B_3)-1}F(1/2) + \frac{(|z_3|/z_2)+1}{(B_1/B_3)-1}$$
$$(B_1>B_3) \quad (14)$$

$$-G(1/2) > \frac{(z_1/z_2)(B_1/B_3)+(|z_3|/z_2)}{1-(B_1/B_3)}F(1/2) + \frac{1+(|z_3|/z_2)}{1-(B_1/B_3)}$$
$$(B_1<B_3) \quad (15)$$

Since the right side of Eq. 15 is positive, the reverse diffusion of the 2 ion can occur, if $B_1<B_3$, only in the case of counter diffusion, that is, in the case where the concentration gradients of the 1 and 2 cations are in the opposite direction so that $G(1/2)<0$.

Equation 14 will be fulfilled if $G(1/2)$ is large enough or if $F(1/2)$ is small enough and (B_1/B_3) is large enough, while Eq. 15 will be fulfilled if $-G(1/2)$ is large enough or if $F(1/2)$ is small enough and (B_1/B_3) is small enough. Therefore, both Eqs. 14 and 15 predict that the reverse diffusion of the 2 cation will be observed when the coexisting cation, 1, is at a smaller concentration but is of a greater concentration gradient and when the mobility of the coexisting cation, 1, differs more from that of the anion, 3.

This may be interpreted as follows: If the coexisting cation, 1, moves faster than the anion, 3, as in the case of Eq. 14, the diffusion potential is generated in such a way that the front part of the diffusion layer is positive and the rear part negative, so that the 2 cation is pulled back by this electric potential, even against its concentration gradient, if the latter is not very large. On the other hand, if the coexisting cation 1 moves much slower than the anion, 3, as in the case of Eq. 15, the direction of the diffusion potential will be opposite to the previous case, so that the 2 cation is pushed forth by this potential, irrespective of the direction of its concentration gradient; the reverse diffusion of the 2 cation results if the direction of its concentration gradient is opposite to those of the 1 cation and the anion, 3.

As for the reverse diffusion of the anion, 3, D'_3 of Eq. 10c or 13 becomes negative when Eq. 16 or 17 is fulfilled, where the use of the suffix 1 for the cation of greater mobility does not lose any generality:

$$1>-G(1/2)>\frac{\{(z_2/|z_3|)+1\}+\{(z_1/|z_3|)(B_1/B_2)+1\}F(1/2)}{\{(B_1/B_2)+(z_2/|z_3|)\}+\{(z_1/|z_3|)+1\}(B_1/B_2)F(1/2)}$$
$$(B_1>B_2) \quad (16)$$

$$-G(1/3)>\frac{\{(z_2/|z_3|)+1\}+\{(z_1/|z_3|)(B_1/B_2)+1\}F(1/2)}{\{(B_1/B_2)-1\}\{1+F(1/2)\}}$$
$$(B_1>B_2) \quad (17)$$

According to Eqs. 16 and 17, it may be concluded that the reverse diffusion of the anion, 3, may be observed only when the concentration gradient of the faster cation, 1, is in the direction opposite to those of the coexisting cation, 2, and of the anion, 3.

Numerical Calculations on the HCl–$CaCl_2$–H_2O System. The numerical values of D'_i have been calculated for

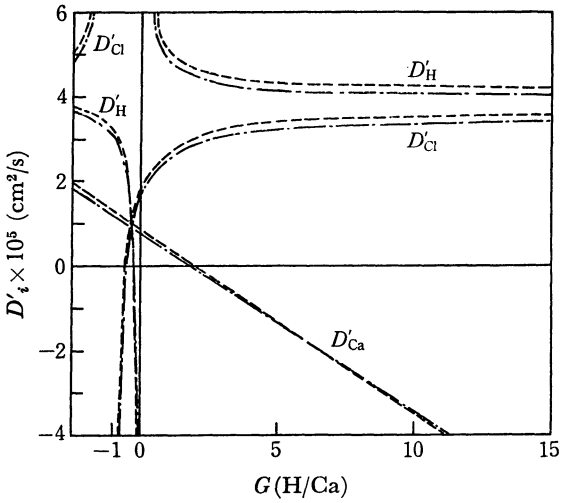

Fig. 1. Calculated values of D'_i against $G(H^+/Ca^{2+})$ at $F(H^+/Ca^{2+})=2$.
The broken lines indicate the values at $h_i=1$, while chain lines indicate the values obtained by using the Güntelberg equation.

the HCl–$CaCl_2$–H_2O system according to Eqs. 10a—d, with 1=H^+, 2=Ca^{2+} and 3=Cl^-. The results for the case of $F(H/Ca)=2$ as an example are shown in Fig. 1, where the concentration-gradient ratio $G(H/Ca)$ is taken on the abscissa.

The broken lines in Fig. 1 are the results obtained for $h_i=1$ by neglecting the concentration dependence of the activity coefficient, while the chain lines are the results obtained by using Eq. 4 and the Güntelberg approximation:[8]

$$\ln f_i = -Az_i^2\sqrt{J}/(1+\sqrt{J}) \quad (18)$$

where A is a constant at a given temperature:

$$A = \sqrt{2\pi N_A/1000}\cdot(e/\sqrt{D_0kT})^3 \quad (19)$$

Here, N_A is the Avogadro Number, e is the elementary charge, D_0 is the dielectric constant of the solvent, and J is the ionic strength:

$$J = (1/2)\sum_i z_i^2[i] \quad (20)$$

By comparing these curves, it may be concluded that the effect of the concentration dependence of the activity coefficient is small, at least in the concentration range studied in this paper.

The values of mobility, B_i, used in these calculations were obtained from the values of the equivalent conductance at an infinite dilution, λ^0_i, given in the literature[9], according to the well-known equation:

$$B_i = \lambda_i^\circ N_A/(|z_i|F_A^2) \quad (21)$$

The values of kTB_i and kTB_ih_i thus obtained are shown in Table 1.

Table 1. Values of D_i ($=kTB_ih_i$) in aqueous HCl–$CaCl_2$ solutions at 25 °C

Ion	λ_i° ($\Omega^{-1}\cdot cm^2\cdot g\text{-}eq^{-1}$)	$D_i\times10^5$ ($cm^2\cdot s^{-1}$)	
		($h_i=1$)	(Güntelberg)
H^+	349.82	9.315	8.990
Ca^{2+}	59.50	0.792	0.682
Cl^-	76.35	2.033	1.928

For the HCl–$CaCl_2$–H_2O system, Fig. 1 shows that the diffusion coefficients, D'_H, D'_{Ca}, and D'_{Cl}, become negative in their respective regions, so that each ion would cause a reverse diffusion in these regions. Figure 1 shows that D'_{Ca} decreases linearly with $G(H/Ca)$, as is to be expected from Eqs. 10b, d, and that D'_{Ca} becomes negative when $G(H/Ca)$ is greater than a certain value, as is to be expected from Eq. 14, since $B_H>B_{Cl}$, as is shown in Table 1.

Figure 1 also shows that the change in D'_H with $G(H/Ca)$ is hyperbolic, as is to be expected from Eqs. 10a, d, and that D'_H becomes negative in the region, which can be expected from Eq. 15a, since $B_{Ca}<B_{Cl}$, as is shown in Table 1. The region of $G(1/2)$, in which D'_1 is negative in the presence of the 2 cation, is derived readily from Eq. 15:

$$0<-G(1/2)<F(1/2)\Big/\left\{\frac{(z_2/z_1)(B_2/B_3)+|z_3|/z_1}{1-(B_2/B_3)}+\frac{1+(|z_3|/z_1)}{1-(B_2/B_3)}F(1/2)\right\} \quad (B_2<B_3) \quad (15a)$$

Instead of $G(H/Ca)$, however, if $G(Ca/H)$ is taken on the abscissa, as is shown in Fig. 5, D'_H is linear, as is to be expected from Eqs. 10b, d, with 1=Ca^{2+} and 2=H^+, and becomes negative when $-G(Ca/H)$ is greater than a certain value, as is to be expected from Eq. 15.

As for the Cl^- anion, the curves shown in Fig. 1 are hyperbolic, as is to be expected from Eqs. 10c, d, with 1=H^+, 2=Ca^{2+}, and 3=Cl^-. The value of D'_{Cl} becomes negative, as is shown in Fig. 1, in the region where $G(H/Ca)$ is negative but greater than -1, as is expected from Eq. 16, since $B_H>B_{Cl}$, as is shown in Table 1. If, however, $G(H/Cl)$ is taken on the abscissa, as is shown in Fig. 6, D'_{Cl} is linear at a fixed value of $F(H/Ca)$, as is to be expected from Eq. 13, and becomes negative when $-G(H/Cl)$ is large enough, as is to be expected from Eq. 17, since $B_H>B_{Cl}$.

Experimental

Diffusion Measurements. McBain's porous-plate method[10] was used for the diffusion measurements, with a diffusion cell modified as has been reported previously.[11] A glass cell divided into two compartments by a porous plate, as is shown in Fig. 2, was held vertically in a thermostat at 25±0.1 °C after each compartment had been filled with a mixed solution of HCl and $CaCl_2$. The solution with the higher density was placed in the upper compartment, I, and that with the lower density, in the lower one, II, in order to keep the concentration distribution in each compartment homogenous by means of convectional flow.[10]

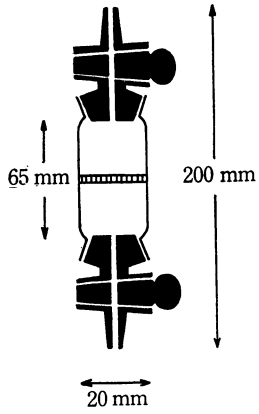

Fig. 2. Diffusion cell.

After a certain time, t, had passed, the concentration in each compartment was measured, and the practical diffusion coefficient, D_i', defined by Eq. 6, was calculated according to the following equations:

$$D_i' = (\langle m_i\rangle/Kt)/\langle[i]_I-[i]_{II}\rangle \quad (22)$$

where K is the cell constant, which depends on the porosity, area, and thickness of the porous plate, and where

$$\langle m_i\rangle = (1/2)\{V_I([i]_I^\circ-[i]_I^t)+V_{II}([i]_{II}^t-[i]_{II}^\circ)\} \quad (23)$$

$$\langle[i]_I-[i]_{II}\rangle = (1/2)\{([i]_I^\circ-[i]_{II}^\circ)+([i]_I^t-[i]_{II}^t)\} \quad (24)$$

where $[i]_I^\circ$ and $[i]_{II}^\circ$ are the initial concentrations of the ion, i, in the upper and lower compartments, $[i]_I^t$ and $[i]_{II}^t$ are those after the time, t, and V_I and V_{II} are the volumes of the compartments.

The diffusion time, t, was set at about 30 h. The values

Table 2. Constants of the diffusion cells used

Cell No.	V_I (ml)	V_{II} (ml)	K (cm)
1	6.9994	7.1516	0.626_1
2	6.4548	6.3961	0.404_5
3	6.6927	6.7142	0.553_4

of V_I and V_{II} are given in Table 2 together with the values of K measured with 0.05 N KCl, the diffusion coefficient of the latter being 1.863×10^{-5} ($cm^2 \cdot s^{-1}$), as is given in the literature.[12]

For the solutions containing only one electrolyte, the diffusion equation (6) can be integrated to obtain the equation to be used for the calculation of the diffusion coefficient.[2,5,11] Instead of this, however, the average amount of diffusion, $\langle m_i \rangle$, and the average concentration difference, $\langle [i]_I - [i]_{II} \rangle$, were used in this study, and the diffusion coefficient was calculated by means of Eq. 22, because the integration with time is complicated for mixed electrolyte solutions.[7] The discrepancy between the diffusion coefficients obtained by Eq. 22 and the usual integrated equation was not more than 10% for the one-electrolyte solutions used.

Parameter Values. In order to compare the experimental D_i' values with the theoretical ones, the values of $F(i/j)$ and $G(i/j)$ defined by Eqs. 11 and 12 are needed. The experimental values of $F(i/j)$ were calculated from:

$$F(i/j) = |z_i/z_j| \cdot \frac{([i]_I^\circ + [i]_{II}^\circ) + ([i]_I^t + [i]_{II}^t)}{([j]_I^\circ + [j]_{II}^\circ) + ([j]_I^t + [j]_{II}^t)} \quad (25)$$

where $([k]_I^\circ + [k]_{II}^\circ)$ and $([k]_I^t + [k]_{II}^t)$, k being i or j, take almost the same values, since V_I and V_{II} have almost the same value. The value of $F(i/j)$ is, therefore, kept almost contant during the diffusion experiment. For the experimental values of $G(i/j)$, the following equation was used with Eq. 24, since the concentration distribution in a diffusion layer had been found to be almost linear:[7]

$$G(i/j) = |z_i/z_j| \langle [i]_I - [i]_{II} \rangle / \langle [j]_I - [j]_{II} \rangle \quad (26)$$

Concentration Determination. The concentration of the H^+ ion was determined by titration with NaOH as the standard solution and with phenolphthalein as the indicator. The concentration of the Ca^{2+} ion was determined by chelatometry, with disodium-EDTA as the standard solution and Eriochrome Black T as the indicator. The concentration of the Cl^- ion was determined by precipitation titration, with $AgNO_3$ as the standard solution and fluorescein as the indicator.

Results and Discussion

Examples of Reverse Diffusion. Some examples of the data are shown in Table 3. Since the parameter values of the three cells used in the experiments are not the same, as is shown in Table 2, the values of $|z_i|[i]_I$ and $|z_i|[i]_{II}$ differ from cell to cell; only the average values are given in Table 3 in order to shorten the listing. The values of D'_i given in the Table are the averages of the values obtained for individual cells. A comparison of data for different cells is given in Figs. 3—6.

It may be seen from Table 3 that the reverse diffusion actually takes place; that is, the concentration increases in the solution with the higher concentration and decreases in that with the lower concentration, for Ca^{2+} in Example 1, for H^+ in Example 2, and for Cl^- in Example 3; the diffusion coefficients, D'_i, are negative in all these cases.

Table 3. Examples of data on the reverse diffusion

Ion	t (h)	$\lvert z_i\rvert[i]_I$ (mN)	$\lvert z_i\rvert[i]_{II}$ (mN)	$D'_i\times10^5$ ($cm^2 \cdot s^{-1}$)
		Example 1		
H^+	0	148.6	52.1	3.66
	30	125.8	74.5	
Ca^{2+}	0	52.6	48.4	−2.68
	30	53.7	47.1	
Cl^-	0	200.7	100.4	3.15
	30	179.7	121.3	
		Example 2		
H^+	0	97.2	103.3	−3.31
	30	94.8	105.7	
Ca^{2+}	0	100.5	0	0.87
	30	93.6	6.8	
Cl^-	0	197.8	103.0	1.29
	30	188.5	112.2	
		Example 3		
H^+	0	87.8	111.6	2.85
	30	92.4	107.0	
Ca^{2+}	0	65.4	35.3	1.05
	30	63.0	37.8	
Cl^-	0	153.1	146.8	−3.06
	30	155.3	144.6	

Reverse Diffusion of Ca^{2+}. The experimental D'_{Ca} values are plotted against G(H/Ca) in Fig. 3 for F(H/Ca) $=0.5$, 1, and 2. This figure also shows that the deviation of the experimental data due to the use of different cells is not large.

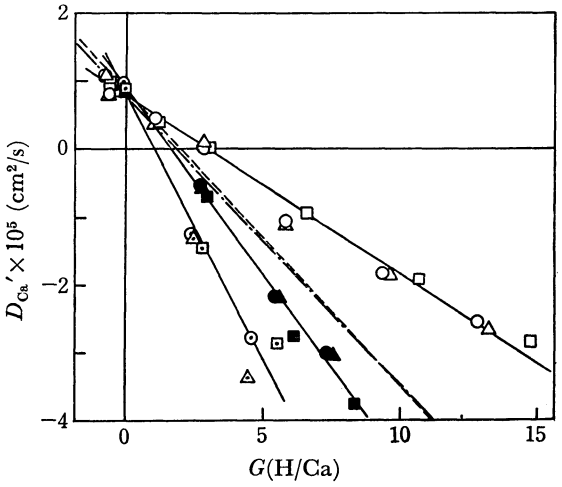

Fig. 3. Diffusion coefficient of Ca^{2+} at 25 °C as a function of G(H/Ca) when F(H/Ca) is fixed.
F(H/Ca)=0.5 (Cell #1, ⊙; #2, ⊡; #3, △), 1.0 (#1, ●; #2, ■; #3, ▲), and 2.0 (#1, ○; #2, □; #3, △).
Theoretical values for F(H/Ca)=2 are shown by a broken line for $h_i=1$, and by a chain line for Güntelberg approximation.

Figure 3 gives the experimental verifications of the theoretical conclusions that D'_{Ca} will be linear to G(H/Ca) and that the inclination will be the steeper when the value of F(H/Ca) is the smaller, as is to be expected from Eqs. 10b, d, with 1=H^+, 2=Ca^{2+}, and

3=Cl^-, and that the reverse diffusion of Ca^{2+} will proceed when G(H/Ca) is large, as is to be expected from Eq. 14.

The theoretical curves for F(H/Ca)=2 are also shown in Fig. 3. Neither of the theoretical curves fits in quantitatively with the experimental straight lines. This will be discussed later. It is, however, noticeable that the experimental results are in agreement, qualitatively, with the theoretical expectations mentioned above.

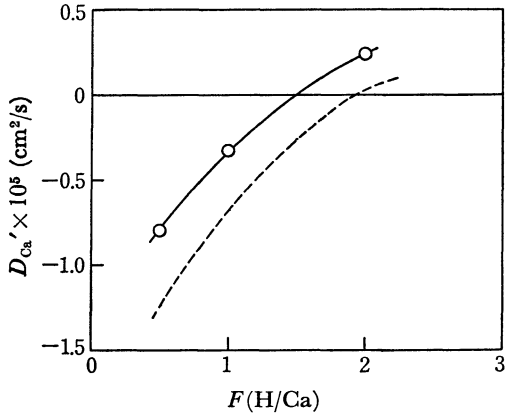

Fig. 4. Dependency of D_{Ca}' on F(H/Ca) for G(H/Ca)=2 at 25 °C.
The broken line is theoretical for $h_i=1$.

The dependency of D'_{Ca} on F(H/Ca) is shown in Fig. 4 for G(H/Ca)=2, where the experimental values are obtained by the interpolation of Fig. 3. It may be seen from Fig. 4 that the experimental curve satisfies qualitatively the trend of the theoretical broken line drawn for $h_i=1$. This result verifies that the reverse diffusion of Ca^{2+} takes place when F(H/Ca) is small, as is to be expected from Eqs. 10b, d.

Reverse Diffusion of H^+ and Cl^-. The dependency of D'_H on G(Ca/H) is shown in Fig. 5 for F(H/Ca)=2, that is, for F(Ca/H)=0.5. The results verify the theoretical conclusions that D'_H will be linear to G(Ca/H) at a fixed F(Ca/H), according to Eqs. 10b, d with

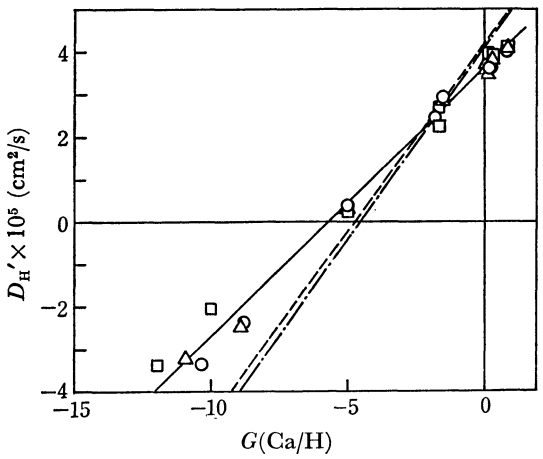

Fig. 5. Dependency of D_H' on G(Ca/H) for F(H/Ca)=2 at 25 °C.
Cell #1, ○; #2, □; #3, △.
Theoretical curves are shown by a broken line for $h_i=0$ and by a chain line for Güntelberg approximation.

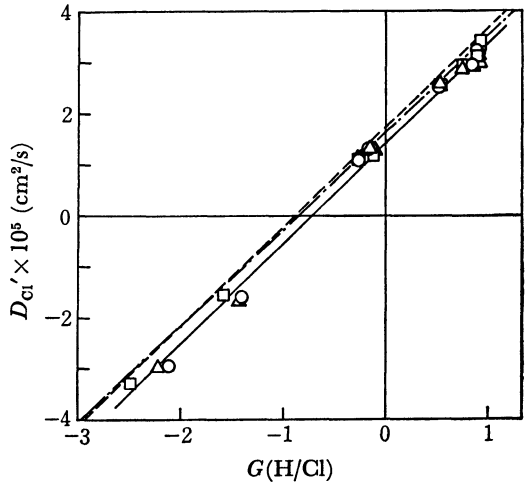

Fig. 6. Dependency of D'_{Cl} on G(H/Cl) for F(H/Ca)=2 at 25 °C.
Cell #1, ○; Cell #2, □; Cell #3, △.
Theoretical curves are shown by a broken line for $h_i=0$ and by a chain line for Güntelberg approximation.

1=Ca^{2+} and 2=H^+, and will be negative when $-G$-(Ca/H) is large, according to Eq. 15, where $B_{Ca}<B_{Cl}$, as is shown in Table 1. The theoretical curves shown in Fig. 5 show the same trend as the experimental results.

The result for D'_{Cl} against G(H/Cl) shown in Fig. 6 is quite similar to that shown in Fig. 5. The relation is linear at a fixed F-value, F(H/Ca)=2, as is to be expected from Eq. 13, and D'_{Cl} becomes negative when $-G$(H/Cl) is large, as is to be expected from Eq. 17, where $B_H>B_{Ca}$, as is shown in Table 1. The discrepancy between experimental and theoretical lines is not large in this case.

Approximation of a Constant Cation Ratio. In our previous papers,[2,4] theoretical equations have been derived, and compared with experimental data, by assuming the fraction of the cation concentrations to be constant throughout the diffusion layer. For a mixed electrolyte solution containing 1 and 2 cations and an anion, 3, the fraction of the equivalent concentration of the 2 cation, ξ_2, defined by:

$$\xi_2 = z_2[2]/(z_1[1]+z_2[2]) \tag{27}$$

may be used in place of $F(1/2)$ and $G(1/2)$ in Eqs. 10a—d, since

$$F(1/2) = G(1/2) = (1-\xi_2)/\xi_2 \tag{28}$$

according to the present assumption. Then, the following equation, which has been given in our previous paper,[4] is obtained:

$$D_2' = kTB_2\frac{(z_1-z_2)B_1(1-\xi_2)+(z_2+|z_3|)B_3}{z_1B_1(1-\xi_2)+z_2B_2\xi_2+|z_3|B_3} \tag{29}$$

The value of D'_2 becomes negative if $z_2>z_1$ and if ξ_2 is small enough, as is shown by the following equation:

$$\xi_2<1-(B_2/B_1)(1+|z_3|/z_2)/(1-z_1/z_2) \quad (z_1<z_2) \tag{30}$$

As for the HCl–$CaCl_2$–H_2O system, the experimental values of D'_i against average ξ_2-values are shown in Fig. 7, together with theoretical broken lines. It may be seen from Fig. 7 that the diffusion coefficient of the slower cation, D'_{Ca}, decreases, both experimentally

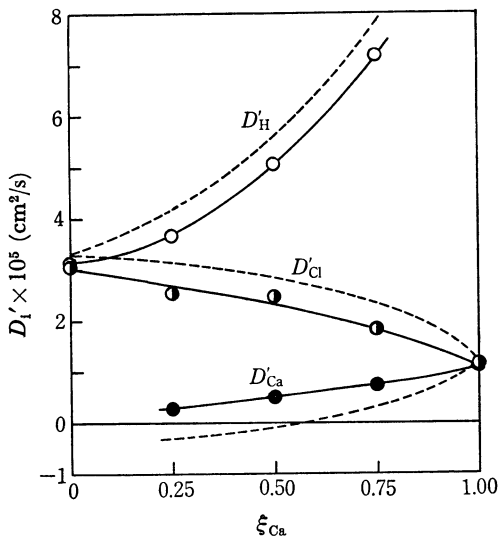

Fig. 7. Relation between D'_i and ξ_{Ca} for aqueous HCl–$CaCl_2$–H_2O solutions at 25 °C.
Experimental data for H^+, ○; Ca^{2+}, ●; Cl^-, ◑.
Broken lines are theoretical for $h_i=1$.

and theoretically, with the decrease in ξ_{Ca}, and that the theoretical curve goes down to negative, as has already been stated,[2,4] although the experimental data do not. This is because the condition $F(1/2)=G(1/2)$ in Eq. 28 is too severe for the accuracy of the present experiments, as may seen from Figs. 3 and 4, which show that D'_{Ca} takes distinctly negative values only in the region where $G(H/Ca)$ is larger than $F(H/Ca)$.

Phenomenological Coefficients. The phenomenological equations of the nonequilibrium thermodynamics are often written as follows for a mixed solution of two electrolytes, A and B[2,3,7,13]:

$$\left.\begin{aligned}[J_A] &= -D_{AA}\left(\frac{\partial[A]}{\partial x}\right)-D_{AB}\left(\frac{\partial[B]}{\partial x}\right)\\ [J_B] &= -D_{BA}\left(\frac{\partial[A]}{\partial x}\right)-D_{BB}\left(\frac{\partial[A]}{\partial x}\right)\end{aligned}\right\} \quad (31)$$

where x is the coordinate in the direction of the diffusion. If the A electrolyte consists of the 1 cation and the anion, 3, and the B electrolyte consists of the 2 cation and the anion, 3, the phenomenological coefficients, D_{AA}, D_{AB}, D_{BA}, and D_{BB}, are related to the mobilities of ions, B_i, according to Eq. 1, since

$$\begin{aligned}&[J_1] = \nu_1[J_A], \quad [J_2] = \nu_2[J_B]\\ &[1] = \nu_1[A], \quad [2] = \nu_2[B]\end{aligned} \quad (32)$$

where ν_1 and ν_2 are the numbers of the respective cations contained in one mole of the electrolytes. The results are given by Eqs. 24—27 of Ref. 7.

This treatment is, however, rather formalistic, because what really exist in the solution of strong electrolytes are not the electrolytes, A and B, but the ions, 1, 2, and 3. For each ion, the phenomenological equation may be written as follows:

$$[J_i] = \sum_j L_{ij}(\partial[j]/\partial x) \quad (33)$$

According to Eq. 1, therefore,

$$\begin{aligned}L_{ii} &= -D_i\\ L_{ij} &= z_i z_j B_i D_j [i]/(\sum_k z_k^2 B_k[k])\end{aligned} \quad (34)$$

If, however, the phenomenological equations are written on the basis of the physico-chemical potentials of the ions, $\tilde{\mu}_i$, as in the following equation,[14]

$$[J_i] = -\sum_j l_{ij}(\partial\tilde{\mu}_j/\partial x) \quad (35)$$

then Eq. 1 corresponds to the case of $l_{ij}=0$ $(i\neq j)$. This means that the cross terms have not yet been taken into consideration, even though the L_{ij} of Eq. 34 and the D_{AB} and D_{BA} of Eq. 31 are not zero.

The possibility that the cross terms, l_{ij}, are not zero might be important in explaining the discrepancy seen in the quantitative comparisons between the theoretical and experimental results, as shown in Figs. 3—7 of this paper. In order to discuss this point further, however, the experimental problems which are related to taking the averages of the concentration gradients between the initial and final values must be settled first, although these expedients do not affect the facts that ions migrated from the lower to the higher concentrations and that the reverse diffusion was actually observed experimentally. Further studies will be reported separately.

References

1) This paper was presented at the 27 th Symposium on Colloid and Interface Chemistry, Akita, October 1974.
2) M. Nakagaki and M. Kobayashi, *Nippon Kagaku Kaishi*, **1973**, 635.
3) R. Flemming and L. J. Gosting, *J. Phys. Chem.*, **77**, 2371 (1973).
4) M. Nakagaki, "Zoku Seitaimaku to Makutoka", ed. by M. Nakagaki, Nankodo Co., Tokyo (1974), p. 1.
5) M. Nakagaki and M. Kobayashi, *Yakugaku Zasshi*, **92**, 1212 (1972).
6) M. Nakagaki, "Yakubutsu no Seitainai Iko", ed. by M. Nakagaki, Nankodo Co., Tokyo (1969), p. 1.
7) M. Nakagaki and M. Kobayashi, *Yakugaku Zasshi*, **93**, 287 (1973).
8) E. Güntelberg, *Z. Phys. Chem.*, **123**, 199 (1926).
9) G. C. Benson and A. R. Gordon, *J. Chem. Phys.*, **13**, 470, 473 (1945); Cf. "Landolt-Börnstein Tabellen", Vol. 2, Part 7, Springer-Verlag, Berlin, Göttingen, Heidelberg (1960), p. 257.
10) J. W. McBain and T. H. Liu, *J. Am. Chem. Soc.*, **53**, 59 (1931). *Cf.* also, J. W. McBain, "Colloid Science", D. C. Heath and Co., Boston (1950), p. 201.
11) M. Nakagaki, N. Koga, and S. Iwata, *Yakugaku Zasshi*, **82**, 1134 (1962).
12) R. H. Stokes, *J. Am. Chem. Soc.*, **73**, 3527 (1951).
13) P. J. Dunlop and L. J. Gosting, *J. Am. Chem. Soc.*, **77**, 5238 (1955); R. L. Baldwin, P. J. Dunlop and L. J. Gosting, *ibid.*, **77**, 5235 (1955); H. Fujita and L. J. Gosting, ibid., **78**, 1099 (1956); P. J. Dunlop, *J. Phys. Chem.*, **61**, 994 (1957); R. P. Wendt, *ibid.*, **69**, 1227 (1965); J. L. Duda and J. S. Vrentas, *ibid.*, **69**, 3305 (1965); and so forth.
14) D. G. Miller, *J. Phys. Chem.*, **71**, 616 (1967).